

Ferromagnetic spin correlations in a few-fermion system

P. O. Bugnion and G. J. Conduit

Cavendish Laboratory, J. J. Thomson Avenue, Cambridge CB3 0HE, United Kingdom

(Received 11 April 2013; published 28 June 2013)

We study the spin correlations of a few fermions in a quasi-one-dimensional trap. Exact diagonalization calculations demonstrate that repulsive interactions between the two species drives ferromagnetic correlations. The ejection probability of an atom provides an experimental probe of the spin correlations. With more than five atoms trapped, the system approaches the itinerant Stoner limit. Losses to Feshbach molecules are suppressed by the discretization of energy levels when fewer than seven atoms are trapped.

DOI: [10.1103/PhysRevA.87.060502](https://doi.org/10.1103/PhysRevA.87.060502)

PACS number(s): 67.85.Lm, 03.65.Ge, 03.65.Xp

Recent experimental advances allow investigators to confine up to twenty atoms in a single trap and address their quantum state [1,2]. This precise control enabled the Heidelberg group to confirm the fundamental physics of short-range repulsion [4–15]. Here we demonstrate that just such repulsive interactions acting between a few fermions allows us to construct a Hamiltonian analogous to the Stoner model [16] and offers experimentalists an opportunity to observe the emergent ferromagnetic correlations without losses to Feshbach molecules.

The itinerant ferromagnet predicted by the Stoner Hamiltonian has never been cleanly realized and studied in the solid state. However, it was proposed [17–19] that a ferromagnetic phase could be created with a fermionic cold atom gas. An experiment by the MIT group displayed signatures compatible with ferromagnetism [20–22], but the observations were later explained by a loss mechanism [23–25]. To circumvent losses it has been suggested that magnetic correlations could be explored in systems with a mass imbalance [26], two-dimensional geometry [27], spin spirals [28], or flux lattices [29]. Here we demonstrate how a quasi-one-dimensional system containing only a few fermions could avoid the problems associated with losses and display ferromagnetic correlations. Our main result is shown in Fig. 1: The discretization of energy levels in the few-fermion system means that losses to Feshbach molecules are restricted to a narrow range of interaction strengths, allowing a tunneling measurement of the ejection of an atom to expose the underlying ferromagnetic correlations.

In this Rapid Communication we first describe the proposed experimental setup, then demonstrate the emergence of ferromagnetic correlations that we study through a tunneling process. Finally, we show that the formation of the competing dimer state is inhibited by the discretization of the energy levels in the harmonic confining potential.

I. EXPERIMENTAL SETUP

A fermionic gas of two hyperfine states with pseudospin $\sigma \in \{\uparrow, \downarrow\}$ is tightly confined as shown in Fig. 1. We seek to solve the Hamiltonian $\hat{H} = \sum_i [-\hbar^2 \nabla_i^2 / 2m + m\omega_{\perp}^2 (x_i^2 + y_i^2) / 2 + m\omega_{\parallel}^2 z_i^2 / 2] + \sum_{i < j} V(\mathbf{r}_i - \mathbf{r}_j)$, with m the atomic mass and $\mathbf{r}_i = (x_i, y_i, z_i)$ the position of atom i . The confining potential is axially symmetric with trap frequencies $\omega_{\perp} = 10\omega_{\parallel}$ [2,3], and we define the harmonic oscillator lengths $a_i = \sqrt{2\hbar/m\omega_i}$. Only a single transverse

mode is occupied, constraining the atoms into the quasi-1D regime. We therefore reparametrize the interspecies potential $V(\mathbf{r}) = -U\Theta(R - |\mathbf{r}|)$ first into the s -wave scattering length $a_{3D} = R[1 - \tan(\chi)/\chi]$ with $\chi = R\sqrt{mU}/\hbar$, and then as a one-dimensional pseudopotential [30] $g = \hbar^2 a_{3D} / ma_{\perp} (a_{\perp} - Ca_{3D})$ with $C = \zeta(1/2) \approx 1.46$. A confinement-induced resonance emerges at $a_{3D} = a_{\perp} / C$. We verified that the results tend to the contact limit below $R = 0.2a_{\parallel}$. In the limit $\omega_{\parallel} \rightarrow 0$, we recover the Stoner Hamiltonian $\hat{H} = \sum_i [-\hbar^2 / 2m (\partial^2 / \partial z_i^2) + m\omega_{\parallel}^2 z_i^2 / 2] + \sum_{i < j} g\delta(z_i - z_j)$.

To probe the quantum state we apply a magnetic field gradient to tilt the external potential (see Fig. 1) and allow one atom to escape. We denote the number of trapped spins N_{\uparrow} and N_{\downarrow} . Investigators can directly measure the spin in the quantization direction $S_z = (N_{\uparrow} - N_{\downarrow}) / 2$ and the total number of atoms $N_{\uparrow} + N_{\downarrow}$ in the final state using the single atom addressability [2]. However, our measure of ferromagnetic correlations, the spin $\mathbf{S} = \langle \sum_n (c_{n\uparrow}^{\dagger} c_{n\downarrow}^{\dagger}) \cdot \sigma \cdot (c_{n\uparrow} c_{n\downarrow})^T \rangle$, is SU(2) invariant, where σ denotes the vector of Pauli-spin matrices and $c_{n\sigma}$ is the annihilation operator of an atom of spin σ from harmonic oscillator state n . Therefore, the spin quantum number defined through $s(s+1) = \langle \mathbf{S}^2 \rangle$ is a good quantum number, allowing us to define the quantum state $|s, N_{\uparrow}, N_{\downarrow}\rangle$. With two atoms a polarized $s = 1$ state can be generated not only from the $S_z = 1$ state, denoted $|1, 2, 0\rangle$, but also from the $S_z = 0$ state denoted $|1, 1, 1\rangle$, corresponding to the prototypical triplet states $|\uparrow\uparrow\rangle$ and $(|\uparrow\downarrow\rangle + |\downarrow\uparrow\rangle) / \sqrt{2}$. The unpolarized $S_z = 0$ state, denoted $|0, 1, 1\rangle$, corresponds to the singlet state $(|\uparrow\downarrow\rangle - |\downarrow\uparrow\rangle) / \sqrt{2}$.

II. ENERGY OF STATES

Our main tool to study the system is exact diagonalization. We build a one-atom basis from the Gaussian orbitals $\phi_{n_x, n_y, n_z}(x, y, z)$ of the harmonic trapping potential. We retain all orbitals that satisfy $(n_x, n_y) \leq 2$ and $n_z \leq 20$. We construct the Slater determinants and select the 10 000 determinants with lowest noninteracting energy, guaranteeing convergence of the energy of the open channel within $0.005\hbar\omega_{\parallel}$. This is much smaller than the energy scale of magnetization, $N_{\uparrow}N_{\downarrow}\hbar\omega_{\parallel}$, and less than the energy difference from the true itinerant state shown in Fig. 2(f). We next calculate the interaction matrix elements numerically, construct the Hamiltonian matrix for a particular g using the Slater-Condon rules, and diagonalize it to obtain the eigenstates $\{\psi_m(g)\}$.

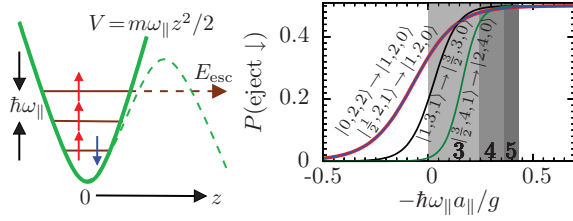


FIG. 1. (Color online) Left: The green solid line is the trapping potential $V(z)$ that is lowered to the green dashed line to allow an atom to escape. The energy levels for up-spin (red) and down-spin (blue) atoms within the potential are shown in brown, with the putative escape of the highest energy up-spin atom. Right: The ejection probability of a down-spin atom into a state fully polarized along the quantization axis. The gray region is excluded due to atom losses for differing initial numbers of atoms.

Exact diagonalization is restricted to systems of fewer than five atoms. However, the experimental setup can contain up to twenty atoms so to analyze the general many-body case we use the QMC code CASINO [31,32]. The approach is a refinement of that used in previous studies of ferromagnetism [20,33–37]. We use a trial wave function $\psi = FD$ that is a product of a Jastrow factor F and a Slater determinant, $D = \hat{A}\{\prod_{i \in n_{\uparrow}} \phi_{n_z}(\mathbf{r}_i)\} \hat{A}\{\prod_{i \in n_{\downarrow}} \phi_{n_z}(\mathbf{r}_i)\}$, where \hat{A} is the antisymmetrization operator. The orbitals are chosen to give the correct noninteracting state on either side of the confinement-induced resonance. The Slater determinant accounts for fermion statistics while the Jastrow factor includes further interparticle correlations. To study the open channel and avoid occupation of the bound state we use the lowest-order constrained variational method [38,39] that is common in nuclear physics and has also been used to study cold atom gases [36,37,40,41]. This method solves the Hamiltonian $[-d^2/dr^2 + mV(r)]rf(r) = k^2rf(r)$. For low-energy s -wave scattering this gives $f(r) \approx 1 - a_{3D}/r$ that has a node at the scattering length a_{3D} , and saturates at large distances. To guarantee occupation of the upper branch, this solution is embedded into a Jastrow factor $F = \prod_{i,j} f(|\mathbf{r}_i - \mathbf{r}_j|)$ where \mathbf{r}_i is the position of the i th up-spin and \mathbf{r}_j the j th down-spin [36,37]. In the quasi-one-dimensional setting the transverse confinement does not allow occupation of the bound state in the range of interaction strengths of interest $0.24 \lesssim -\hbar\omega_{\parallel} a_{\parallel}/g < \infty$. The maximum binding energy of the last band to cross the open channel is $\sim -1.5\hbar\omega_{\parallel}$, which is much less than the energy scale of the transverse modes $\sim 20\hbar\omega_{\parallel}$. This was further confirmed by studying the exact diagonalization states, where deep in the super-Tonks regime occupation of the higher transverse modes is $\sim 10^{-7}$, resulting in the strong agreement between exact diagonalization results and QMC demonstrated in Figs. 2(a)–2(d). Meanwhile, to calculate the binding energy of the molecule at $g > 0$ and the ground open channel state at $g < 0$ we use a Jastrow factor $F = e^J$, where J includes the polynomial expansion in atom-atom separation proposed in Ref. [42] with eight variational parameters.

With the exact diagonalization and QMC formalism in place, in Figs. 2(a)–2(d) we compare the ground-state energy predicted by both exact diagonalization and QMC, and also the two-atom exact analytical solution [4,6,7]. There is strong

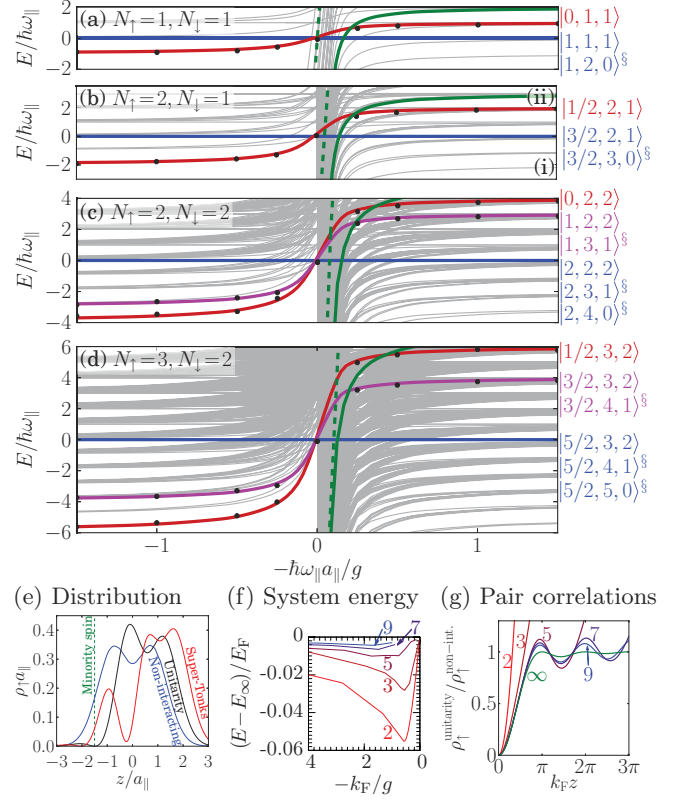


FIG. 2. (Color online) (a)–(d) The energy of the (two–five)-atom states calculated with exact diagonalization. The red, magenta, and blue lines highlight open channels with § signifying identical states with larger S_z , and gray lines indicating all other states. The green line shows the final bound molecular state that crosses the low-spin open channel, and the green dashed line the bound state with the COM motion excited into the $n_{x,y} = 2$ orbital examined in Ref. [13]. The points show QMC results whose uncertainty is the point size. (e) Density profile of the state $|1/2, 2, 1\rangle$ for two majority species atoms with a pinned minority atom. (f) Difference in energy from the polaron in an infinite system [45] with number of trapped atoms. (g) Pair correlation function at the confinement-induced resonance around a down-spin pinned at $z = 0$ normalized by the noninteracting density profile.

agreement at all interaction strengths. The underlying attractive potential means that exact diagonalization also delivers the multitude of molecular bound states and repeated bands incremented by $\hbar\omega_{\parallel}$ corresponding to center-of-mass (COM) motion. In the two-atom system Fig. 2(a), in the noninteracting regime, $-\hbar\omega_{\parallel} a_{\parallel}/g \rightarrow -\infty$, the lower spin state $|0, 1, 1\rangle$ has the lowest energy. At the confinement-induced resonance the spin states cross [2,3], and in the super-Tonks regime, $-\hbar\omega_{\parallel} a_{\parallel}/g \rightarrow \infty$, the $s = 1$ states have lower energy.

In the three-body system in Fig. 2(b) three open-channel states are possible: the low-spin $|1/2, 2, 1\rangle$ and the high-spin states $|3/2, 3, 0\rangle$ and $|3/2, 2, 1\rangle$. Similarly to the two-body system, at weak interactions the $s = 1/2$ state has the lower energy, the bands cross at the confinement-induced resonance, and in the super-Tonks regime the $s = 3/2$ states are favorable, in good agreement with existing literature [9,12]. In Fig. 2(c) we also studied the four-atom case where three values for the

spin are available: $s \in \{0,1,2\}$. The three bands cross at the confinement-induced resonance meaning that any potential onset of ferromagnetism would be abrupt, as occurs in the infinite-body case [43,44]. With five atoms the molecular bands become more prevalent, and we will later demonstrate how they allow losses into bound molecules.

In the super-Tonks regime the high spin state is energetically favorable so the gas would enter the magnetic phase if it were not blocked by spin conservation. However, the spatial distribution of the atoms betrays the underlying magnetic correlations. In the three-atom state $|1/2,2,1\rangle$, we pin the minority down-spin atom at $z = -1.5a_{\parallel}$. In the noninteracting case the up-spin atom density is concentrated around the trap center irrespective of the down-spin position. At the confinement-induced resonance the up-spin density is driven to zero at the down-spin pinning position, whereas in the super-Tonks regime, the up-spin atoms are forced away from the down-spin forming a separate magnetic domain.

Now that we have observed the emergence of magnetic correlations we study the energy of a single down-spin in a trap with N_{\uparrow} majority spin atoms to assess the consequences of system size and whether the system serves as a model for the Stoner Hamiltonian. We compare our system to the analytically solvable polaron limit [45] of a single down-spin in a sea of up-spin atoms. We first study the energy of a polaron in Fig. 2(f). With $N_{\uparrow} = 1$, exact diagonalization displays less repulsion energy than the infinite-body case. On inserting more majority spin atoms the energy quickly tends to the infinite-sized limit [45], being within $\lesssim 1\%$ at all interaction strengths with $N_{\text{tot}} \geq 5$. Second, in Fig. 2(g) we study the pair correlation function. With more majority spin atoms the pair correlation function quickly tends to the infinite-body limit [45], with the correct correlation hole and first Friedel oscillation observed for $N_{\text{tot}} \geq 5$. Both pieces of evidence indicate that systems with $N_{\text{tot}} \geq 5$ are faithful representations of the itinerant Stoner Hamiltonian.

III. TUNNELING STATISTICS

Although the magnetic phase is energetically favorable in the super-Tonks regime its formation is prohibited by spin conservation. In Fig. 1 we therefore tilt the trap to allow one atom to escape. This allows the system to tunnel into the magnetic ground state containing one fewer atom. We calculate the tunneling rate using Fermi's golden rule. The tunneling rate Γ exhibits an exponential dependence on the escape energy, so we need only consider tunneling from the highest occupied orbital with maximal energy E_{esc} . We now consider a general intermediate interaction strength and calculate the probability of forming a particular state i , $p_i = \Gamma_i / \sum_j \Gamma_j$. This tunneling probability calculated from the exact diagonalization data is shown in Fig. 1. We focus on the polaron limit with multiple up-spin atoms and a single down-spin atom.

At zero interactions the highest energy majority spin atom is expelled leading to zero probability of ejecting the minority spin atom, whereas at the confinement-induced resonance all atoms have an equal probability of expulsion. In the super-Tonks regime starting with N_{tot} atoms, the system will tunnel most rapidly into the state with lowest energy—the fully polarized state with $s = (N_{\text{tot}} - 1)/2$. There are two quantum

states available: with $S_z = (N_{\text{tot}} - 1)/2$ formed by the ejection of the down-spin atom and $S_z = (N_{\text{tot}} - 2)/2$ formed by the ejection of an up-spin atom. Starting with three atoms tunneling into a two-atom state, these are simply the triplet states $|\uparrow\uparrow\rangle$ and $(|\uparrow\downarrow\rangle + |\downarrow\uparrow\rangle)/\sqrt{2}$. These two possibilities occur with equal probability, giving a plateau probability of $1/2$ for ejecting a minority spin atom in the super-Tonks regime irrespective of the initial number of atoms. The probability curves in Fig. 1 become increasingly sharp with more atoms because of the larger energy exchange over the same range of interaction strengths.

The tunneling method is sensitive to S_z but not s so does not provide a full diagnosis of the final quantum state. This is exemplified when starting from the polaron state in the super-Tonks regime where the ejection probability of a minority spin is $1/2$ rather than unity. To distinguish the $|1,1,1\rangle$ state from the other possible $S_z = 0$ state, $|0,1,1\rangle$, one could ramp the interaction strength into the noninteracting regime and measure the energy through a second tunneling measurement [2,3]. Should the $|1,1,1\rangle$ state be dominant the energy will be independent of interaction strength, whereas if $|0,1,1\rangle$ dominates, the energy will fall.

IV. LOSS MECHANISM

The search for itinerant ferromagnetism in a cold atom gas has been plagued by a competing loss process [23–25]. Several models for loss have been put forward including two- and three-body models [23,24,46,47], and losses to states excited with transverse COM motion [13–15,25]. To conserve energy, both mechanisms require the open channel to cross molecular bands. Our Hamiltonian only displays avoided crossings between states with the same COM quantum number. However, states with different COM motion could have avoided crossings due to unforeseen perturbations such as an anharmonic potential [13–15,25]. To guarantee a loss-free experiment, we fence off the region in which the open channel is crossed or anticrossed by any other state. This pessimistic approach is robust to unforeseen perturbations that may alter the crossings but will not significantly alter the positions of the bands. We first focus on the three-body system where we use Fig. 2(b) to define a loss region as where the desired open channel $|1/2,2,1\rangle$ crosses the molecular bound states.

The ground molecular bound state labeled (i) is lower than the entire open channel $|1/2,2,1\rangle$ so its formation is prohibited by energy conservation. The molecular bound state can be excited with COM motion, giving rise to increasingly populous families of curves. The curves (ii) are the first set of molecular bands to cross the state $|1/2,2,1\rangle$. Further crossings from more excited molecular bands occur up to the confinement-induced resonance, prohibiting experimentalists from looking for magnetic correlations within $0 \lesssim -\hbar\omega_{\parallel}a_{\parallel}/g \lesssim 0.24$. This region contains the molecular bound state with COM motion excited into the second transverse mode that is a significant cause of loss in an anharmonic potential [13–15,47]. Though the definition of g used to characterize the interaction strength does not conform to the correct effective pseudopotential for the excited transverse states [48], it properly describes the experimentally relevant ground transverse states.

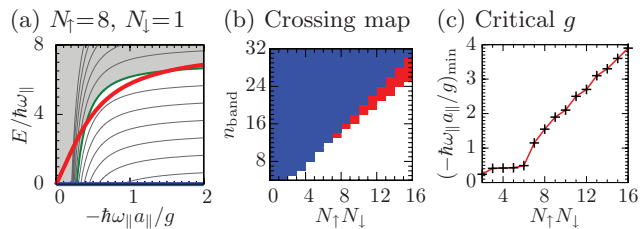


FIG. 3. (Color online) (a) The energy bands, following Fig. 2 conventions. (b) The map of crossing events for the n_{band} -th excited molecular state with $N_{\uparrow}N_{\downarrow}$. Blue denotes a single crossing, and red a double crossing. (c) The minimum interaction strength to avoid the band crossing region.

We note that it is possible to adiabatically transit across the region of band crossing. Investigators can perform experiments on the $|1/2, 2, 1\rangle$ state either side of the shaded region in Fig. 1, but not within it. A similar analysis of a system with four atoms reveals that losses would block the region $0 \lesssim -\hbar\omega_{\parallel}a_{\parallel}/g \lesssim 0.36$, and with five atoms the range $0 \lesssim -\hbar\omega_{\parallel}a_{\parallel}/g \lesssim 0.42$.

Exact diagonalization cannot accurately address larger systems. We therefore turn to QMC for the open channel and the variational QMC for the molecular band. In the super-Tonks regime the energy difference between unpolarized and polarized states is $\hbar\omega_{\parallel}N_{\uparrow}N_{\downarrow}$, so we categorize states by $N_{\uparrow}N_{\downarrow}$. We focus on the state that bounds the loss region, with the molecule having no COM motion, and other atoms in higher energy orbitals compatible with the correct noninteracting energy. With $N_{\uparrow}N_{\downarrow} = 2$ in Fig. 2(b) the excited

molecule bands cross the upper branch only once, whereas with $N_{\uparrow}N_{\downarrow} = 8$ in Fig. 3(a) a molecular band, highlighted in green, crosses the open channel twice. In Fig. 3(b) we show whether the n_{band} -th family of excited molecular bands crosses the open channel once or twice. The double crossings first emerge at $N_{\uparrow}N_{\downarrow} = 7$ and become ubiquitous as $N_{\uparrow}N_{\downarrow}$ rises. This leads to a proliferation in the total number of band crossings, and as shown in Fig. 3(c) a dramatic rise in the minimum interaction strength $-\hbar a_{\parallel}\omega_{\parallel}/g$ required to avoid band crossings.

V. DISCUSSION

A quasi-one-dimensional system containing a few fermionic atoms poses an opportunity to explore ferromagnetic correlations. Discretization of the energy levels offers the stabilization of a ferromagnetic state without losses. We have calculated the energy structure and studied the ejection probabilities. Both the polaron energy and pair correlation function tend to the itinerant limit when $N_{\text{tot}} \geq 5$, whereas molecule losses restrict the observation of magnetic correlations to $N_{\text{tot}} \leq 6$. Therefore, systems with $N_{\text{tot}} \in \{5, 6\}$ could present an opportunity to observe magnetic correlations driven by the Stoner mechanism.

ACKNOWLEDGMENTS

The authors thank Gerhard Zürn, Thomas Lompe, Selim Jochim, and Stefan Baur for useful discussions. P.O.B. acknowledges the financial support of the EPSRC and G.J.C. the support of Gonville and Caius College.

-
- [1] P. Cheinet, S. Trotzky, M. Feld, U. Schnorrberger, M. Moreno-Cardoner, S. Fölling, and I. Bloch, *Phys. Rev. Lett.* **101**, 090404 (2008).
 - [2] F. Serwane, G. Zürn, T. Lompe, T. B. Ottenstein, A. N. Wenz, and S. Jochim, *Science* **332**, 336 (2011).
 - [3] G. Zürn, F. Serwane, T. Lompe, A. N. Wenz, M. G. Ries, J. E. Bohn, and S. Jochim, *Phys. Rev. Lett.* **108**, 075303 (2012).
 - [4] M. Rontani, *Phys. Rev. Lett.* **108**, 115302 (2012).
 - [5] D. Rubeni, A. Foerster, and I. Roditi, *Phys. Rev. A* **86**, 043619 (2012).
 - [6] Z. Idziaszek and T. Calarco, *Phys. Rev. A* **74**, 022712 (2006).
 - [7] T. Busch, B.-G. Englert, K. Rzǎzewski, and M. Wilkens, *Found. Phys.* **28**, 549 (1998).
 - [8] C. Mora, R. Egger, A. O. Gogolin, and A. Komnik, *Phys. Rev. Lett.* **93**, 170403 (2004).
 - [9] I. Brouzos and P. Schmelcher, arXiv:1209.2891.
 - [10] X.-J. Liu, H. Hu, and P. D. Drummond, *Phys. Rev. A* **82**, 023619 (2010).
 - [11] J. Rotureau, arXiv:1302.4301.
 - [12] S. E. Gharashi, K. M. Daily, and D. Blume, *Phys. Rev. A* **86**, 042702 (2012).
 - [13] S. Sala, G. Zürn, T. Lompe, A. N. Wenz, S. Murmann, F. Serwane, S. Jochim, and A. Saenz, arXiv:1303.1844.
 - [14] E. L. Bolda, E. Tiesinga, and P. S. Julienne, *Phys. Rev. A* **71**, 033404 (2005).
 - [15] V. S. Melezhik and P. Schmelcher, *New J. Phys.* **11**, 073031 (2009).
 - [16] E. C. Stoner, *Proc. R. Soc. London, Ser. A* **165**, 372 (1938).
 - [17] R. A. Duine and A. H. MacDonald, *Phys. Rev. Lett.* **95**, 230403 (2005).
 - [18] G. J. Conduit and B. D. Simons, *Phys. Rev. A* **79**, 053606 (2009).
 - [19] L. J. LeBlanc, J. H. Thywissen, A. A. Burkov, and A. Paramekanti, *Phys. Rev. A* **80**, 013607 (2009).
 - [20] G. J. Conduit and B. D. Simons, *Phys. Rev. Lett.* **103**, 200403 (2009).
 - [21] G.-B. Jo *et al.*, *Science* **325**, 1521 (2009).
 - [22] G. J. Conduit, A. G. Green, and B. D. Simons, *Phys. Rev. Lett.* **103**, 207201 (2009).
 - [23] D. Pekker *et al.*, *Phys. Rev. Lett.* **106**, 050402 (2011).
 - [24] C. Sanner, E. J. Su, W. Huang, A. Keshet, J. Gillen, and W. Ketterle, *Phys. Rev. Lett.* **108**, 240404 (2012).
 - [25] E. Haller *et al.*, *Phys. Rev. Lett.* **104**, 153203 (2010).
 - [26] C. W. von Keyserlingk and G. J. Conduit, *Phys. Rev. A* **83**, 053625 (2011).
 - [27] G. J. Conduit, *Phys. Rev. A* **82**, 043604 (2010).
 - [28] G. J. Conduit and E. Altman, *Phys. Rev. A* **82**, 043603 (2010).
 - [29] S. K. Baur and N. R. Cooper, *Phys. Rev. Lett.* **109**, 265301 (2012).
 - [30] M. Olshanii, *Phys. Rev. Lett.* **81**, 938 (1998).

- [31] R. Needs, M. Towler, N. Drummond, and P. López Ríos, CASINO version 2.3 User Manual, Cambridge University, 2008; W. M. C. Foulkes, L. Mitas, R. J. Needs, and G. Rajagopal, *Rev. Mod. Phys.* **73**, 33 (2001).
- [32] R. J. Needs, M. D. Towler, N. D. Drummond, and P. López Ríos, *J. Phys.: Condens. Matter* **22**, 023201 (2010).
- [33] D. M. Ceperley and B. J. Alder, *Phys. Rev. Lett.* **45**, 566 (1980).
- [34] G. Ortiz, M. Harris, and P. Ballone, *Phys. Rev. Lett.* **82**, 5317 (1999).
- [35] F. H. Zong, C. Lin, and D. M. Ceperley, *Phys. Rev. E* **66**, 036703 (2002).
- [36] S. Pilati, G. Bertainia, S. Giorgini, and M. Troyer, *Phys. Rev. Lett.* **105**, 030405 (2010).
- [37] S.-Y. Chang, M. Randeria, and N. Trivedi, *Proc. Natl. Acad. Sci. USA* **108**, 51 (2011).
- [38] V. R. Pandharipande and H. A. Bethe, *Phys. Rev. C* **7**, 1312 (1973).
- [39] V. R. Pandharipande and K. E. Schmidt, *Phys. Rev. A* **15**, 2486 (1977).
- [40] S.-Y. Chang, V. R. Pandharipande, J. Carlson, and K. E. Schmidt, *Phys. Rev. A* **70**, 043602 (2004).
- [41] S. Cowell, H. Heiselberg, I. E. Mazets, J. Morales, V. R. Pandharipande, and C. J. Pethick, *Phys. Rev. Lett.* **88**, 210403 (2002).
- [42] N. D. Drummond, M. D. Towler, and R. J. Needs, *Phys. Rev. B* **70**, 235119 (2004).
- [43] X. Cui and T.-L. Ho, *Phys. Rev. Lett.* **110**, 165302 (2013).
- [44] L. Wang, Z. Xu, and S. Chen, *Eur. Phys. J. D* **66**, 265 (2012).
- [45] J. B. McGuire, *J. Math. Phys.* **6**, 432 (1965).
- [46] D. S. Petrov, *Phys. Rev. A* **67**, 010703(R) (2003).
- [47] S. Sala, P.-I. Schneider, and A. Saenz, *Phys. Rev. Lett.* **109**, 073201 (2012).
- [48] T. Bergeman, M. G. Moore, and M. Olshanii, *Phys. Rev. Lett.* **91**, 163201 (2003).